Article

Current Biology

Rules and Self-Organizing Properties of Post-embryonic Plant Organ Cell Division Patterns

Graphical Abstract

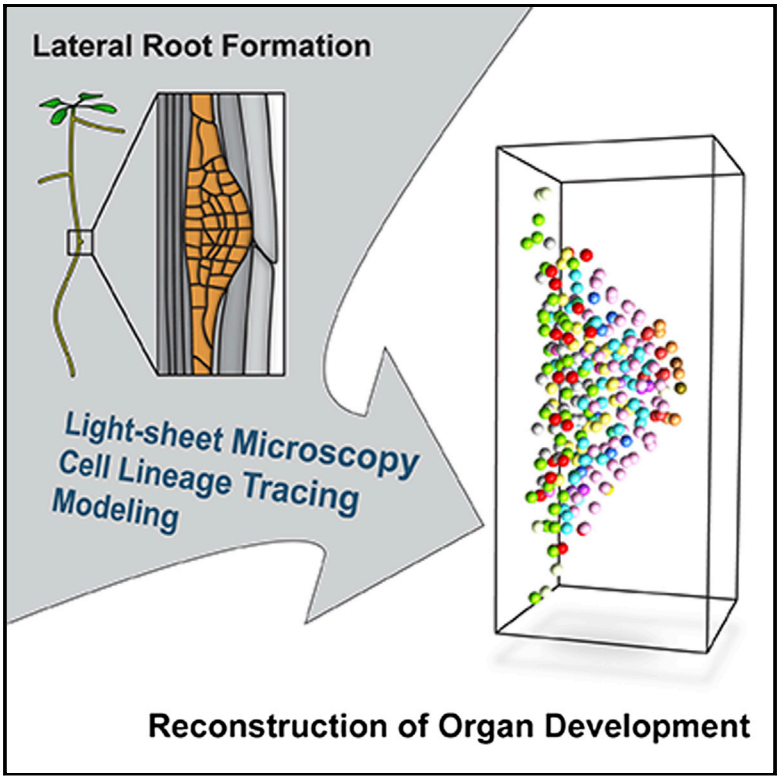

Authors

Daniel von Wangenheim, Jens Fangerau, Alexander Schmitz, Richard S. Smith, Heike Leitte, Ernst H.K. Stelzer, Alexis Maizel

Correspondence

ernst.stelzer@physikalischebiologie.de (E.H.K.S.), alexis.maizel@cos.uni-heidelberg.de (A.M.)

In Brief

von Wangenheim et al. use modeling and light sheet microscopy observations for an in-depth analysis of cell division patterns during lateral root formation in *Arabidopsis*. The orthogonal shifts in division planes and the layered organization of the root can be explained by simple rules that lead to global self-organizing patterns.

Highlights

- The first full four-dimensional atlas of lateral root formation is provided
- The timing of emergence of layers is stereotypic relative to the number of cells
- The contribution of each founder cell to the primordium is not stereotypical
- The initial asymmetric division has long-term effects on division patterns

von Wangenheim et al., 2016, Current Biology *26*, 439–449
February 22, 2016
http://dx.doi.org/10.1016/j.cub.2015.12.047

CellPress

Current Biology
Article

Rules and Self-Organizing Properties of Post-embryonic Plant Organ Cell Division Patterns

Daniel von Wangenheim,[1,5] Jens Fangerau,[2,3] Alexander Schmitz,[1] Richard S. Smith,[4] Heike Leitte,[3] Ernst H.K. Stelzer,[1,*] and Alexis Maizel[2,*]
[1]Buchmann Institute for Molecular Life Sciences, Goethe Universität Frankfurt am Main, 60438 Frankfurt am Main, Germany
[2]Center for Organismal Studies, Heidelberg University, 69120 Heidelberg, Germany
[3]Interdisciplinary Center for Scientific Computing, Heidelberg University, 69120 Heidelberg, Germany
[4]Department of Comparative Development and Genetics, Max Planck Institute of Plant Breeding Research, 50829 Cologne, Germany
[5]Present address: Developmental and Cell Biology of Plants, Institute of Science and Technology Austria, 3400 Klosterneuburg, Austria
*Correspondence: ernst.stelzer@physikalischebiologie.de (E.H.K.S.), alexis.maizel@cos.uni-heidelberg.de (A.M.)
http://dx.doi.org/10.1016/j.cub.2015.12.047

SUMMARY

Plants form new organs with patterned tissue organization throughout their lifespan. It is unknown whether this robust post-embryonic organ formation results from stereotypic dynamic processes, in which the arrangement of cells follows rigid rules. Here, we combine modeling with empirical observations of whole-organ development to identify the principles governing lateral root formation in *Arabidopsis*. Lateral roots derive from a small pool of founder cells in which some take a dominant role as seen by lineage tracing. The first division of the founders is asymmetric, tightly regulated, and determines the formation of a layered structure. Whereas the pattern of subsequent cell divisions is not stereotypic between different samples, it is characterized by a regular switch in division plane orientation. This switch is also necessary for the appearance of patterned layers as a result of the apical growth of the primordium. Our data suggest that lateral root morphogenesis is based on a limited set of rules. They determine cell growth and division orientation. The organ-level coupling of the cell behavior ensures the emergence of the lateral root's characteristic features. We propose that self-organizing, non-deterministic modes of development account for the robustness of plant organ morphogenesis.

INTRODUCTION

A hallmark of organismal development is the establishment of robust organ morphologies through controlled growth. Organs are characterized by typical patterns of cell organization and differentiation. Because plant cells are turgid, immobile, and feature a cell wall, cell growth determines plant organ shape and cell division orientation influences cell disposition. In *Arabidopsis*, early embryogenesis specifies the apical-basal axis as well as the root and shoot meristems. This highly stereotypic process is characterized by a nearly invariant pattern of cell divisions [1–3]. However, post-embryonic development with formation of lateral organs is the main determinant of a plant's architecture and its unparalleled ability to adapt [4, 5]. It remains unknown whether the strict determinisms that underpin the arrangement of cells during embryogenesis also apply to morphogenesis of post-embryonic lateral organs. In roots, lateral organs are derived from patches of founder cells that are semi-regularly specified in the differentiation zone [6]. In *Arabidopsis*, the lateral root founders are cells of the pericycle, a single inner cell layer adjacent to the vascular bundle at the center of the root [7]. Small numbers of pericycle cells re-enter the cell cycle and divide anticlinal (along the shoot-root axis) and periclinal (normal to the surface of the root) to form a dome-shaped primordium that further progresses into a lateral root. The primordium grows through the cell layers of the primary root [8], which accommodate the passage and have an instructive role in the initiation [9] and shape of the lateral root primordium [10]. As it develops, the lateral root primordium adopts a characteristic organization in cell layers [11].

RESULTS

A Geometric Rule for Division Accounts for the Tissue Organization of the Lateral Root Primordium

Quantitative analyses and modeling have established that, for most plant cell divisions, the division plane is coupled to a "shortest wall" principle [1, 12–14]. This has been shown to be true for proliferative divisions in the early *Arabidopsis* embryo, where only divisions in which daughter cells adopt a different fate tend to break this rule [1]. We tested whether the same principle accounts for the emergence of the typical cell organization of the early lateral root primordium. We developed a growing, two-dimensional vertex-based model of the formation of the lateral root to evaluate whether the regular organization of cells in the lateral root primordium can emerge with a limited set of rules. Our model assumes an initial arrangement of founder cells in the pericycle. Growth is simulated by morphing this initial configuration into the shape of a fully developed lateral root primordium (Figures 1A and S7) using a key-framing approach

based on Bézier surfaces [15]. The simulated shape change captures both the growth of the primordium itself and the accommodating responses of the overlying tissue [8–10, 16]. As the cells grow, their area increases, and at a threshold area (or area ratio), they divide. Different rules determine the orientation of the plane of division (e.g., geometric shortest wall), and the choice of division rule will influence the patterning of the cells in the developed primordium. We simulated the formation of lateral roots assuming a coupling between the orientation of the plane of division and cell geometry. We implemented a probabilistic rule, in which the selection of the plane of division involves a competition between configurations that represent local minima (geometric, shortest wall rule) [14]. Because of the probabilistic nature of this rule, we ran 100 simulations of the model and analyzed a combined output. All simulations lead to the formation of a layered primordium, which resembles the cellular organization observed in actual lateral root primordia (Figures 1A and S7). The layered organization of cells in the primordium arises from periclinal divisions [11]. We noticed the emergence of higher-order spatial and temporal regularities in the sequence of periclinal divisions. Once two layers (an inner and an outer layer) are generated by a periclinal division, the outer layer predominantly shows periclinal divisions prior to the inner layer (Figure 1B). We also analyzed the sequence of cell divisions and correlated the spatial orientation between two consecutive divisions. We computed the planar angle ɵ between the axis of the n^{th} cell division and the $n\text{-}1^{th}$ cell division. We observed that most cells rotated their division plane by 90° (Figure 1C). Two spatial domains are observed in the model. A central domain composed of small cells flanked by a peripheral domain with larger cells [17] is observed (Figure 1A). Therefore, a model in which divisions follow a geometric rule for positioning of the plane of division recapitulates the tissue organization of the lateral root primordium. The model allows several predictions about the cell organization and the division pattern of the lateral root primordium. First, the order of periclinal divisions should be regular, with periclinal divisions occurring in the outer layer prior to the inner layer. Second, two consecutive divisions should predominantly switch the division plane orientation by 90°.

A Four-Dimensional Atlas of Cell Lineages during Lateral Root Formation

To rigorously test these predictions in vivo, it is crucial to analyze cell movements, divisions, and lineage relationships of cells [18, 19]. Previous attempts to document and reconstruct the lineages of cells forming the lateral root primordium [10, 20] lacked the dynamics or temporal resolution for a faithful inference of the lineages of all cells. To perform a comprehensive study of all cell lineages involved in lateral root morphogenesis, we employed light sheet-based fluorescence microscopy (LSFM) [21–25]. LSFM allows in vivo recording of the complete process of lateral root formation of transgenic *Arabidopsis thaliana* plants expressing a pan-nuclear marker (pUBQ10::H2B-RFP) and a pan-plasma membrane marker (pUBQ10::YFP-PIP1;4) for up to 3 days without photo-bleaching while leaving the plant intact. The observed plants expressed furthermore a nuclear reporter (pGATA23::nls-GUS-GFP) specifically marking the pericycle cells primed to become founder cells [26]. Thereby, we ensured that the recording starts prior to the first cell division. All plants were imaged in a customized microscope [23], allowing a fine control of simulated sun light intensity, temperature, and the availability of nutrients. As a result, we precisely reproduce the standard growth conditions, in which *Arabidopsis* plants are commonly grown in laboratories [23]. Initially, the 7-day-old plants were gravistimulated by a 90° rotation for a period of 6 hr (Figure S1). This treatment induces the formation of lateral roots [27, 28] and provides a common reference time point. Given the plastic nature of post-embryonic development, it is essential to sample the inter-individual variance in cell behavior. Therefore, we captured the complete morphogenesis of five lateral root primordia in five different plants grown under identical conditions (Figures 1D, 1E, and S1; Tables 1 and S1). In each recording, stacks of images were acquired every 5 min for up to 64 hr. We did not observe any adverse effects on the plants during the imaging process. The plants survived imaging, showed no morphological abnormalities, and continued their normal life cycle past imaging (Figure S1). The LSFM datasets document the positions of all cells forming the lateral root and allow the visualization and analysis of lateral root morphogenesis at cellular resolution (Figures 1E and S1; Movies S1 and S2). We define three canonical views of lateral root morphogenesis (Figure 1E). In the front view, the primordium grows toward the observer; the side view runs along the shoot/root axis with the primordium growing sideways from the primary root axis. In the radial view, the primordium is cut transversally by a plane perpendicular to the shoot/root axis. We took advantage of the high spatiotemporal resolution of our datasets to track cell nuclei through multiple rounds of cell division and generated a comprehensive database of positions and lineage relationships for all cells of the lateral root primordium (Figure S2). We tracked all nuclei for 25 hr, a time window spanning the lateral root formation from the first division of the founders in the pericycle layer to the emergence of the primordium through cortex and epidermis layers. The resulting lateral root datasets allowed us to reconstruct the entire lateral root formation process and to perform extensive data analyses (Figures 1F, 1G, and S2; Data S1).

Lateral root founder cells are all pericycle cells that divide at least once during the recording time. We counted 8–15 founder cells (11 ± 2; mean ± SD) arranged in a patch of five to eight parallel pericycle cell files facing the xylem pole (Figure 1F) [11, 29, 30]. These cells are arranged in pairs of abutting pericycle cells. Single cells were also observed at the periphery of the field of founders (Figure S4). The first division of a founder cell is observed 7–14 hr after gravistimulation (10:41 ± 3:10; hh:mm; mean ± SD; Figure 1D). Although each primordium is initiated at a different time point, their growth rates are very similar, following an exponential profile with an average doubling time of 7:08 ± 00:17 hr (mean ± SD; Figures 2A and S1). We did not observe any correlation between the growth rates and the day/night cycle, as it is known to be the case for emerged lateral roots [23, 31]. Due to the large variance in the onset of proliferation after gravistimulation, we analyzed the different datasets based on the total number of cells in the primordium for a developmental synchronization of our system. This allows a direct comparison of the five datasets at particular developmental stages up to a number of 143 cells. The timing of development and the typical emergence of a layered organization were consistent across all datasets and similar to previous reports [10, 11]. We conclude that our datasets

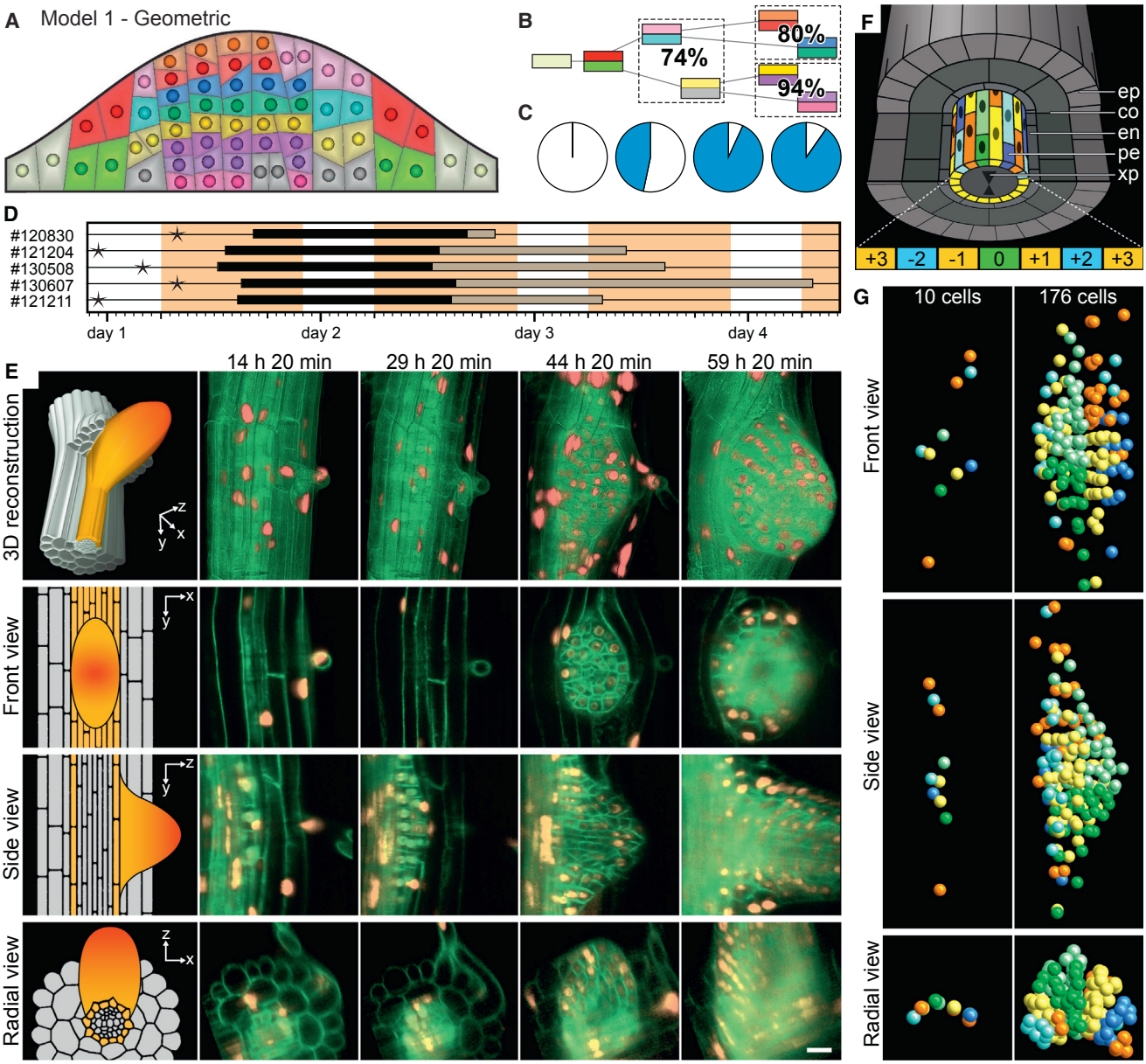

Figure 1. Modeling, Imaging, and Reconstruction of Lateral Root Formation in *Arabidopsis thaliana*

(A) Modeling of lateral root growth using geometric rules of cell divisions. All cells divide symmetrically following the shortest wall rule. Cell outlines overlaid with nuclei show the resulting model at the end of the simulation. Colors indicate layers as in Figure 2D.

(B) Tree representation of the order of periclinal divisions. Percentages indicate the proportion of periclinal divisions that occur in the outer layer prior to the inner layer in 100 independent simulation runs of the model.

(C) Pie charts representing the proportion of alternating divisions (in blue) in 100 independent simulation runs of the model.

(D) Time course of five datasets. The development of each specimen is presented along a line. The star indicates the time point of gravistimulation, the bar shows the entire time span of the recording, and its black segment indicates the period of segmentation and tracking. Daytime and nighttime are represented by an orange and a white background, respectively.

(E) Live recording of lateral root development from initiation to emergence for dataset no. 121204. Schematics in the first column describe the different perspectives on the lateral root. First row: a three-dimensional reconstruction of the lateral root growing out of the primary root is shown. Second row: single slices along x-y (front view), 10 μm inside the epidermis cell layer, are shown. Third row: single slices along z-y (side view), 80 μm inside the primary root, are shown. Fourth row: single slices along x-z (radial view) through the center of the primordium are shown. Time points are relative to gravistimulation. The scale bar represents 20 μm.

(F) Schematic representation of the disposition of the lateral root founder cells in the pericycle. co, cortex; en, endodermis; ep, epidermis; pe, pericycle; xp, xylem pole.

(G) Spatial distribution of cell nuclei in data set no. 120830. The first and last segmented time points are shown in front, side, and radial views. Clonally related cells share the same color. The color scheme follows the one in (F).

See also Figures S1, S2, and S4 and Movies S1 and S2.

Table 1. Samples Imaged and Datasets Analyzed

		Imaging				Segmented Dataset			
Dataset	Genotype	Duration	Frequency	Volume (x, y, z) (μm)	Size of the Dataset (GB)	Duration (hr)	No. of Founders	No. of Cells at the End	No. of Divisions
No. 120830	wild-type	47 hr	every 5 min	443 × 335 × 150	175	25	10	167	166
No. 121204	wild-type	45 hr	every 5 min	443 × 335 × 150	167	25	11	160	156
No. 121211	wild-type	39 hr 30 min	every 5 min	443 × 335 × 150	147	25	11	260	242
No. 130508	wild-type	50 hr 30 min	every 5 min	443 × 335 × 150	188	30	9	143	134
No. 130607	wild-type	65 hr 20 min	every 5 min	443 × 335 × 150	243	25	15	267	252
No. 131203	*aur1-2 aur2-2*	42 hr 55 min	every 5 min	443 × 335 × 150	159	41	5[a]	175[a]	174[a]

[a]Underestimated, as one peripheral cell file could not be analyzed.

accurately reflect lateral root development and faithfully capture the passage through stereotypic stages [10, 11].

Growth Dynamics, Sequence of Periclinal Divisions, and Layers Emergence

Next, we asked whether the observed stereotypic growth of the primordia entails an invariable pattern of growth dynamics in the primordium. For this, we used the nuclei as landmarks to quantify in 3D the dynamics of the tissue deformation in all datasets, which was then averaged (see [32] and Experimental Procedures). From initiation to a primordium of ~70 cells, the principal direction of tissue deformation is uniform throughout the primordium and parallel to the shoot-root axis. Afterward, the axis of deformation rotates by 90° and points toward the surface of the main root (Figure 2B; Movie S3). This rotation is particularly notable in the central and apical parts of the primordium, whereas it stays parallel to the shoot-root axis at the base and periphery of the primordium. In conclusion, the morphogenesis of the lateral root primordium follows a stereotypic pattern characterized by an apical growth.

We then characterized the spatiotemporal elements in the sequence of periclinal divisions accounting for the regular emergence of layers. We observed that the occurrence of periclinal divisions correlates with given developmental stages, i.e., with the number of cells. For example, the first periclinal division occurs at a stage of 26 ± 6 cells and the second periclinal division occurs when the primordium contains 57 ± 6 cells (Figures 2D, 3, and S3). We also observed the higher-order spatial and temporal regularities in the sequence of periclinal divisions predicted by the model. Once two layers (an inner and an outer layer) are generated by a periclinal division, the outer layer predominantly shows periclinal divisions prior to the inner layer (Figures 2D, 3, and S3). Together, this indicates that the emergence of layers results from a stereotypic timing of periclinal divisions relative to the total number of cells in the primordium and a stereotypic distribution relative to its geometry. In turn, this could suggest a control at the scale of the whole primordium.

Founder Cells Do Not Contribute Stereotypically to the Lateral Root Primordium

The swelling of the pericycle cells located in one cell file [9] is a distinctive feature preceding the first founder cell division. This cell file received the index zero and, because it occupies a leading role in the development of the primordium (Figures 4A and 4B), can be regarded as the master cell file. Not only cells in the master cell file are predominantly the first among the founders to enter the first round of division, but also their daughters are the first cells that enter the subsequent rounds of divisions (Figure S4). We measured the duration of the interphase in each cell file and observed that the lineages derived from the master cell file and its immediate flanking neighboring files (with indices −1 and +1) had a shorter interphase duration (6.01 ± 1.83 hr; mean ± SD) than the ones at the periphery (7.17 ± 2.28 hr; $p = 4.724e{-}14$; Welch two-sample t test; Figure 4C). In consequence, cells in the master cell file contribute most of the cell mass in the primordium (31%; 44 ± 6 cells for a primordium at the 143 cells stage; Figure 4D). Together, founders of the master file and its two adjacent files (files −1, 0, and +1) define the core of the primordium and contribute 76% (109 ± 6 cells for a primordium at the 143 cells stage) of the cell mass (Figure 4D). The contribution of individual founder cells is also not comparable from one primordium to the other. For example, at the 143 cells stage, in one specimen (dataset no. 130508), 60% of the primordium consisted of the progeny of two cells, whereas in another specimen (dataset no. 130607), it required five founder cells to create 60% of the primordium (Figure 4E). Thus, all founders do not contribute equally to the primordium, consistent with an earlier cell-sector-based study [20]. We determined the position of the primordium tip in the last time point of the recording in the side view and projected it onto the first time point (Figure 4E) to analyze whether the founder cells determine the position of the primordium tip. We measured the position of the cell borders in each of the cell files −1, 0, and +1 relative to this center. Neither the position of the cells in the master cell files nor the average center of the three central cell files coincides with the position of the center of the primordium (Figures 4E and S4). This leads to the conclusion that the position of the primordium tip is not encoded in the initial position of the founder cells and suggests that there is a considerable extent of plasticity in cell patterning to form a lateral root. The rigid endodermis layer directly overlying the founder cells is actively accommodating the initiation and growth of the primordium [9, 16]. We searched for any conspicuous feature in the arrangement of the overlying endodermis in relation to the position of the founder(s) with a predominant contribution to the primordium. We extracted the topology of the endodermis cell walls and projected the position onto the primordium tip. We observed in all datasets that the founder cell contributing most to the primordium was in contact with two endodermis cells (Figure S4). This result suggests that the topological relationships

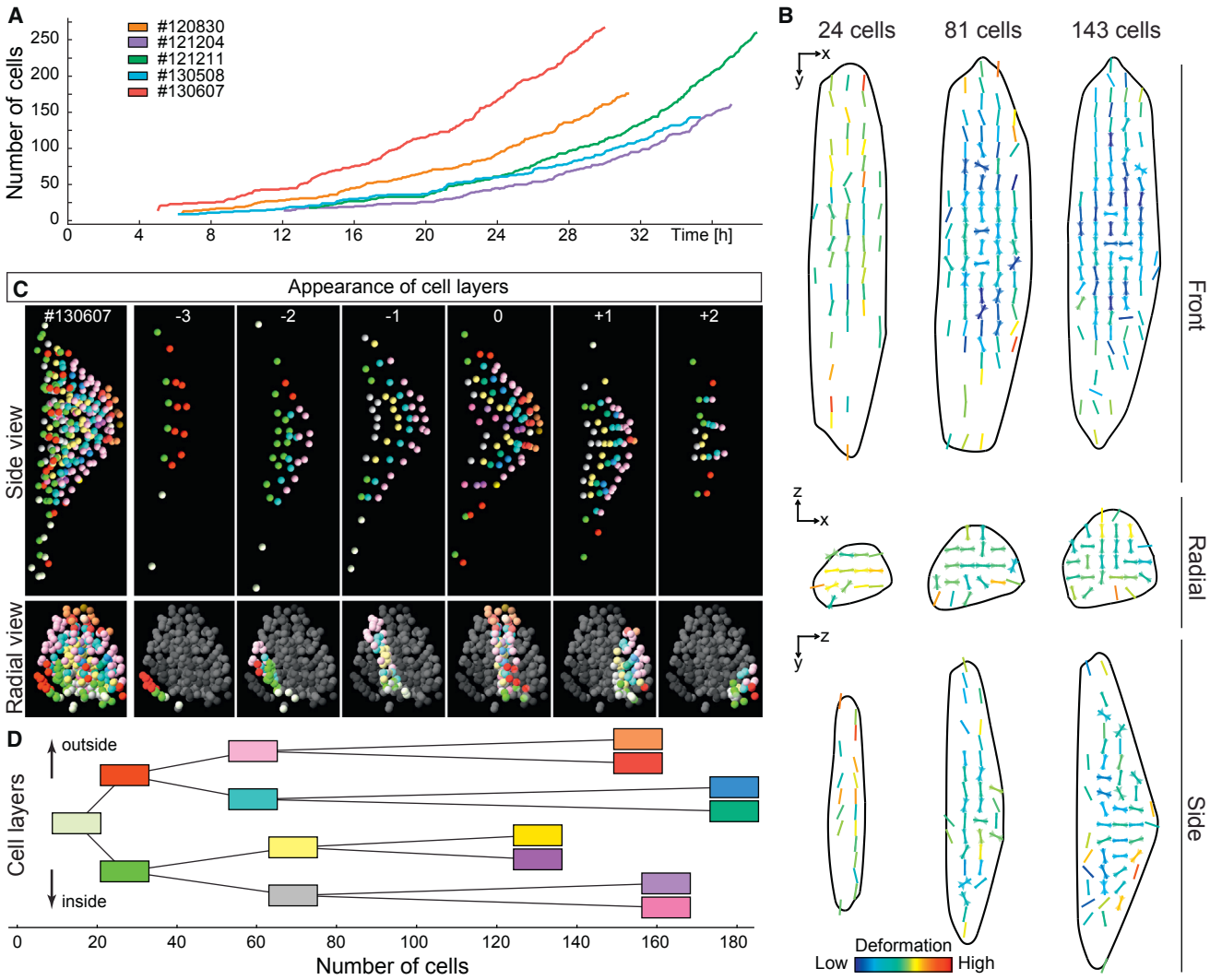

Figure 2. High-Order Regularities in the Growth Profile and the Sequence of Periclinal Divisions

(A) Number of cells over time for all datasets. The horizontal axis indicates the time after gravistimulation.

(B) Average tensor maps of the developing lateral root. The position of the cell nuclei was used to compute the 3D deformation in each individual primordium. The datasets were spatially and temporally registered, and the deformation was averaged over all datasets. These maps reflect the magnitude (color) and principal directions of the growth of the lateral root primordium (line). Three stages are represented as canonical views. Whereas all cells are shown in the radial and front views, only the cells of the master cell file (see Figure 4) are shown in the side view. The "bow ties" represent the variance in orientation. The black line represents the outline of the primordium.

(C) Layer visualization of the dataset no. 130607. The cell nuclei positions in the last segmented time point are shown in the side and radial views. Each column shows the cell nuclei of an individual cell file ranging from index −3 to +2. Colors indicate the sequence of periclinal divisions. Starting from a one-layered primordium, the first periclinal division generates two layers, an outer one (red) and an inner one (green), that undergo further periclinal divisions and generate more layers (see D).

(D) Tree representation of the average sequence of periclinal divisions in all five datasets. The horizontal axis represents the total number of cells in the primordium. The positions of the boxes indicate the average number of cells at which these layers appeared.

See also Figures S2 and S3 and Movies S3 and S4.

between endodermis and pericycle may have a role in the selection of the founder cell with a dominant contribution.

Spatiotemporal Patterns of Cell Division

We then analyzed the spatiotemporal pattern of cell divisions. As previously reported [7, 11, 30, 33], the first division of the founders in the master cell file is stereotypic. Founders undergo an anticlinal (A), asymmetric division generating two small cells flanked by two larger cells. For the second round of divisions, we observed two cases: either cells undergo a periclinal (P) division, thus creating a new layer (AP case; Figure 5A), or they go through another round of anticlinal division (AA case; Figure 5B). Founder cells seem to randomly follow either of the two sequences (AA or AP). This indicates that there might not be a stereotypic division pattern except that the first division is always anticlinal. We then analyzed whether the predicted regular 90°

History of periclinal divisions at given total number of cells							
Dataset	1. periclinal	2. periclinal outer layer	2. periclinal inner layer	3. periclinal outer layer 2	3. periclinal outer layer 1	3. periclinal inner layer 2	3. periclinal inner layer 1
#120830	22	58	66	146	-	119	152
#121204	30	60	73	-	-	147	154
#121211	30	64	89	157	172	145	165
#130508	17	48	56	-	-	-	-
#130607	29	56	55	158	174	102	172
Average	**26**	**57**	**68**	**154**	**173**	**128**	**161**
SD	6	6	14	7	1	22	9

Figure 3. Timing of Periclinal Divisions

For each of the five datasets, the number of cells in the primordium when the first, second, and third periclinal divisions occur is indicated. Starting from a one-layered primordium (pale green), the first periclinal division generates two layers, an outer one (red) and an inner one (green), that undergo further periclinal divisions and generate more layers. See also Figures S2 and S3 and Movie S4.

switch in the axis of two consecutive divisions was also observed in vivo. Between the first and the second division round, 46% of divisions shifted their division plane by 90° (e.g., anticlinal to periclinal), whereas 54% divided along the same direction (Figures 5C and 5D; n = 75 divisions). This bimodal distribution is expected. We previously observed that cells divide first anticlinal and then either switch to a periclinal division (AP case leading to an alternating behavior) or divided again anticlinal (AA case leading to a collinear behavior). In the subsequent rounds of divisions, we observed a net predominance of an alternating orientation between two consecutive divisions (68% alternating; 32% collinear; n = 584; Figure 5C). This indicates that, after the second round of divisions, most of the cells switch the orientation of their plane of division by 90° and show alternating division.

Cell shape is an important determinant of the orientation of cell divisions [1, 13, 14]. We thus analyzed the relationship between the orientation of the divisions and the geometry of the cell and classified the orientation of the new cell wall with respect to the geometry of the mother cell for the first four rounds of divisions. Division planes that split the cell in parallel to its shortest axis follow the shortest wall rule [12, 14]. All divisions in the first round are anticlinal and follow this rule. These divisions follow a shortest wall rule while generating unequal daughter cells, a case reminiscent of the situation observed in the stomatal lineage where the plane of division is the shortest path through the nucleus, but the nucleus is not in the center of the cell [34]. In the second round, only 50% of the divisions follow the shortest wall rule (Figure 5D). For example, some periclinal cell divisions occur although the mother cell is considerably elongated (Figure S5). In contrast, during the third and fourth division rounds, 80% of the divisions obey the shortest wall rule (Figure 5D). In summary, from the third cell cycle onward, cells tend to divide following a geometric rule and alternate their division behavior. Both observations are significantly reduced during the second cell cycle. As predicted by the model, it appears that a particular control of the cell division orientation during the first cell cycle creates a field of small cells that delineate the future primordium center. In order to test this hypothesis, we took advantage of the *aurora1 aurora2* (*aur1-2;2-2*) double mutant that lacks key AURORA kinases required to correctly position the cell plate in asymmetric formative cell divisions [35]. This defect results in a randomized orientation of cell divisions in early stage primordia and leads to a compromised lateral root emergence despite the normal dome shape of the primordium [10]. We recorded the lateral root development of an *aur1-2;2-2* plant expressing ubiquitously a H2B-RFP and PIN1-GFP fusion and retrieved the lineage of founders. As previously reported [10, 35], we observed that, during the early stages of primordium development, the plant is not capable of specifying division planes in the initial two rounds of divisions. This causes an erratic arrangement of the cells (Figures 5E and S6). The primordium establishes still a dome-like shape (Figure 5E) but does not form organized layers (Figure 5F). In contrast to the wild-type, periclinal divisions do not occur in the outer layer prior to the inner layer (Figure 5G), nor do two consecutive divisions alternate the orientation of the division plane during the first four rounds of divisions (Figure 5H). This suggests that the mispositioning of the division plane during the first asymmetrical division of the founders has profound consequences on the tissue organization of the primordium. It prevents the formation of organized layers and the switch in division orientations. Yet, the dome shape of the primordium is not affected.

Our analyses of the developing lateral root primordium validate several predictions of the model. The first anticlinal and asymmetric division of the founders determines the further tissue organization of the primordium. Most divisions tend to switch their division plane by 90° between two consecutive divisions. High-order regularities in the sequence of periclinal divisions lead to the well-organized formation of layers. Yet, our analyses revealed additional characteristic elements that were not predicted by the model. Lateral root primordia develop from a variable number of founder cells from which some arise to have a dominant contribution. These dominant founders seem to arise stochastically. The division pattern of individual founders varies between primordia.

The Orientation of Cell Divisions and the Deformation Pattern of the Primordium Drive Lateral Root Morphogenesis

Our results suggest that the reproducible outcome of lateral root morphogenesis is an emerging property of the orientation

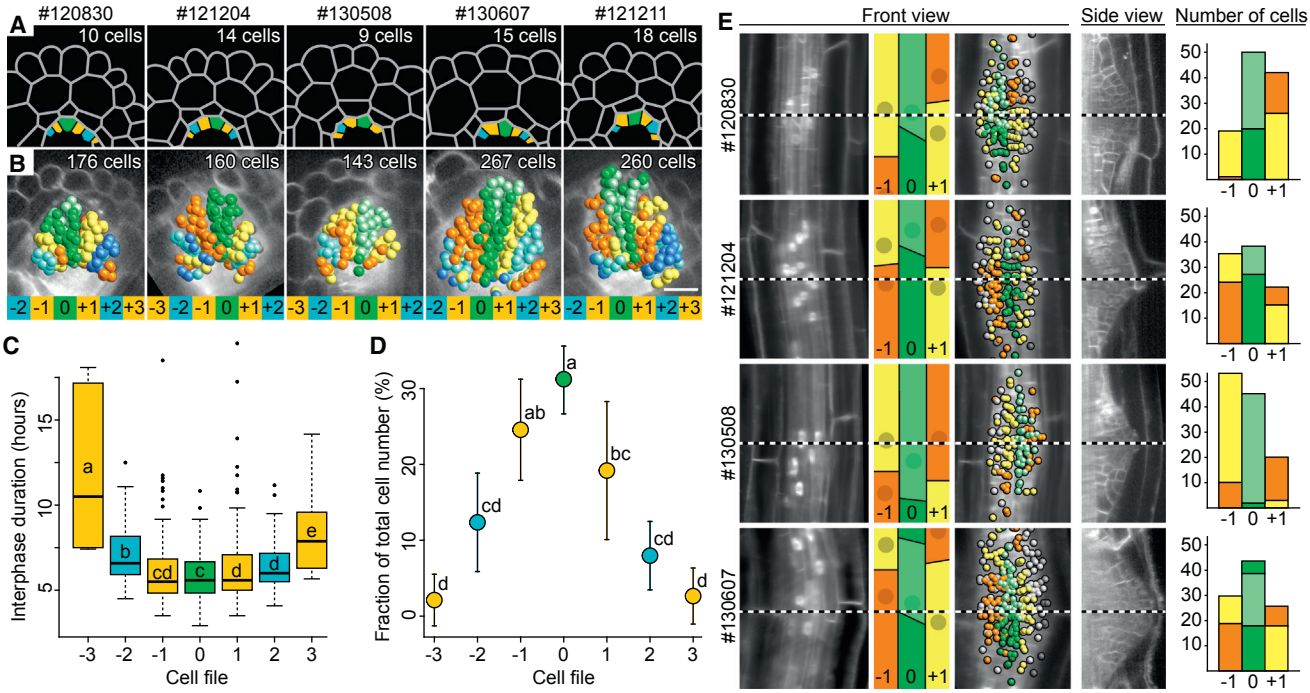

Figure 4. Emergence of a Master Cell File and Non-stereotypic Contribution of Individual Founders

(A) Sketch of the membranes (radial view) at the first time point for all datasets. The cell file swelling the most prior to its first division is called master cell file and indicated in green.

(B) Overlay of the cell nuclei positions and single optical slices through the center of the primordium in radial view at the last segmented time point. The master cell file (index zero) prefigures the tip of the primordium. Flanking cell files on either side have indices ranging from −3, i.e., leftmost, to +3, i.e., rightmost.

(C and D) Cells in the master cell file have a shorter interphase duration and contribute most to the lateral root. (C) Box plots of the time span between two consecutive divisions in each cell file are shown. (D) Fraction of the total cell number (for a 143-cell primordium) derived from each cell file plotted as the mean ± SD over all datasets is shown. In both (C) and (D), identical letters indicate distributions that do not differ significantly ($p \geq 0.05$; Tukey's test).

(E) The disposition of founder cells does not prefigure the position of the tip of the lateral root primordium. Front and side views of four datasets at the first and last segmented time points are depicted along a schematic representation of the founders upon initiation (second column) and an overlay of the nuclei position and single slices in the last segmented time point (third column). The number of cells (for a 143-cell primordium) contributed by founders in each of the three core cell files is indicated in the last column.

See also Figure S4.

of cell divisions and the deformation pattern of the primordium. To formally assess the role of cell division orientation, we randomized the orientation of divisions by treating all possible orientations of the division planes with the same probability. A complete randomization of the division plane could lead to cells with uneven volume distribution between daughter cells, a feature correlated with the formation of daughter cells with distinct identity [1]. Therefore, we ran models in which the orientation of the division plane is randomized while still preserving the symmetry of the daughter cells. In such a model, which mimics the defect of the *aurora* kinase mutant, cells of the primordium did not arrange in layers and no distinct peripheral and central domains emerged (Figures 6D and S7). Because the plane of division was chosen randomly, the predominant alternation between two divisions was no longer present (Figure 6E). These results are qualitatively similar to the defects observed in vivo with the *aurora* mutant. In contrast to the *aurora* mutant data, the high-order pattern of periclinal division was still observed in the model (Figure 6F). We further tested the importance of a precise control of the orientation during the first division. We ran simulations in which the choice of plane of division for the first division is randomized, whereas all subsequent divisions follow a geometric shortest wall rule as in the first model (Figures 6G–6I and S6). In this case, organized layers were not as readily visible (Figure 6G) similar to the *aurora* mutant. In contrast, the alternated division orientation was restored (Figure 6I) and the high-order pattern of periclinal divisions was present (Figure 6H). This result supports the hypothesis that a precise control of the orientation of the first division is an important determinant of emergence of layers. In addition, it suggests that a precise control of the division plane orientation, involving the AURORA kinases, is important for the proper emergence of the sequence of layers as well as for the regular switch in division orientation.

We observe a stereotypic distribution of periclinal divisions relative to the primordium geometry, where these divisions initially occur in the outermost layers. Because this pattern is preserved in models, where the orientation of cell division is randomized, we hypothesize that it results from a global control at the level of the whole primordium. We tested whether the lateral root primordium growth could be responsible for the emergence of this high-order regularity. For this, we changed from a mostly

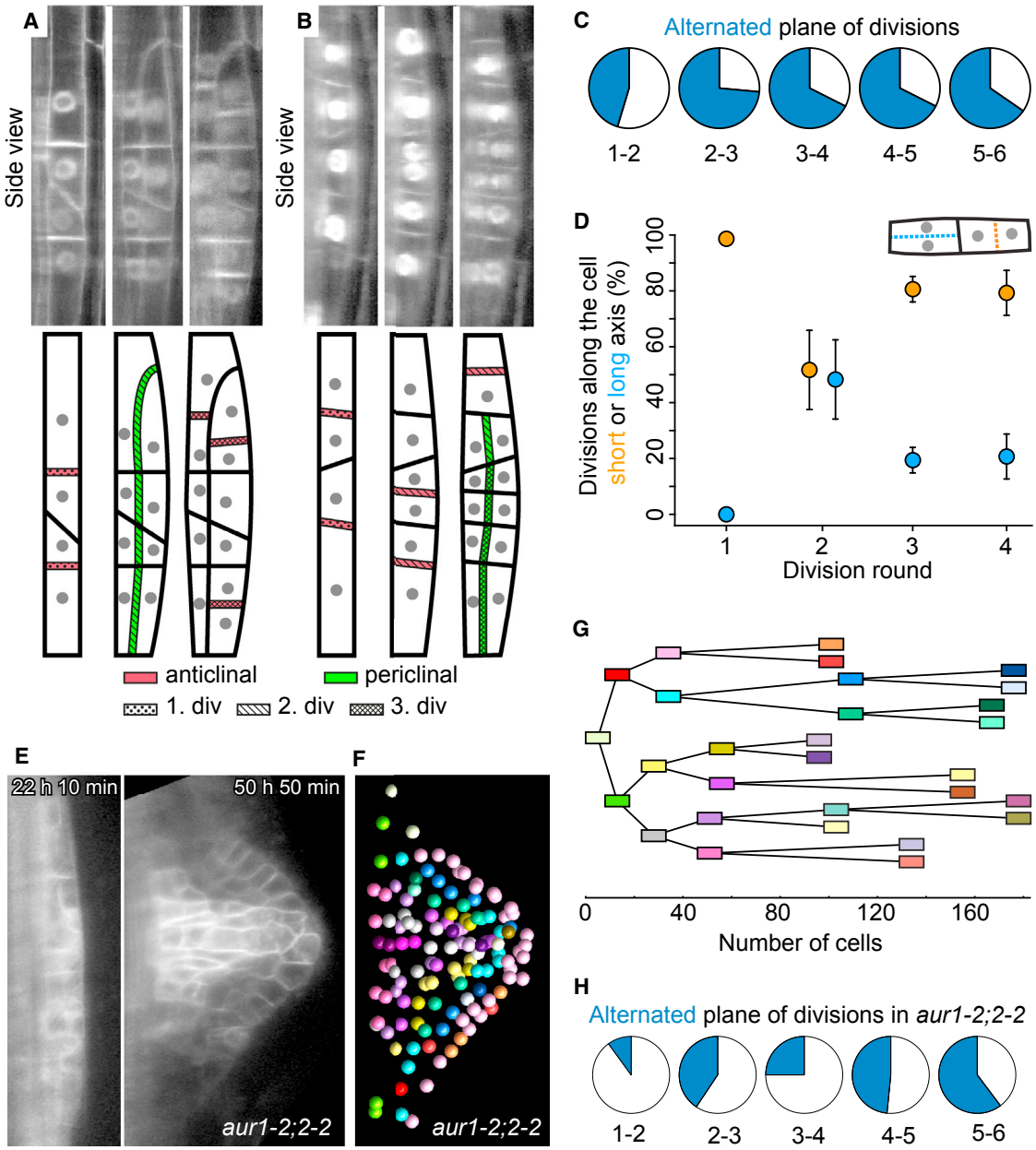

Figure 5. Patterns of Division Orientation during Lateral Root Formation

(A and B) Optical sections through the master cell file (upper part) and schematic representations (lower part) of two primordia taken at three time points during the first three divisions. In (A), the founders first divide anticlinally and then periclinally (AP pattern), whereas in (B), the founders divide either twice anticlinally before their first periclinal division (AA pattern) or follow the AP pattern.

(C) Pie charts show the proportion of alternating divisions (in blue) in the division rounds. All five datasets are considered.

(D) Average proportion of cells in three datasets (nos. 120830, 121204, and 130508; n = 161), which divide along the long (blue) or the short (orange) axis of the cell in the indicated division rounds.

(E–H) Analysis of a lateral root for the aurora kinases double mutant *aur1-2;2-2*.

(E) Optical sections through the master cell file at time points after gravistimulation illustrate the development of the *aur1-2;2-2* mutant.

(F) Layer visualization of the *aurora* mutant dataset.

(G) Tree representation of the sequence of periclinal divisions for the aurora mutant.

(H) Proportion of alternated divisions (in blue) for the indicated division rounds in the aurora mutant.

See also Figures S5 and S6.

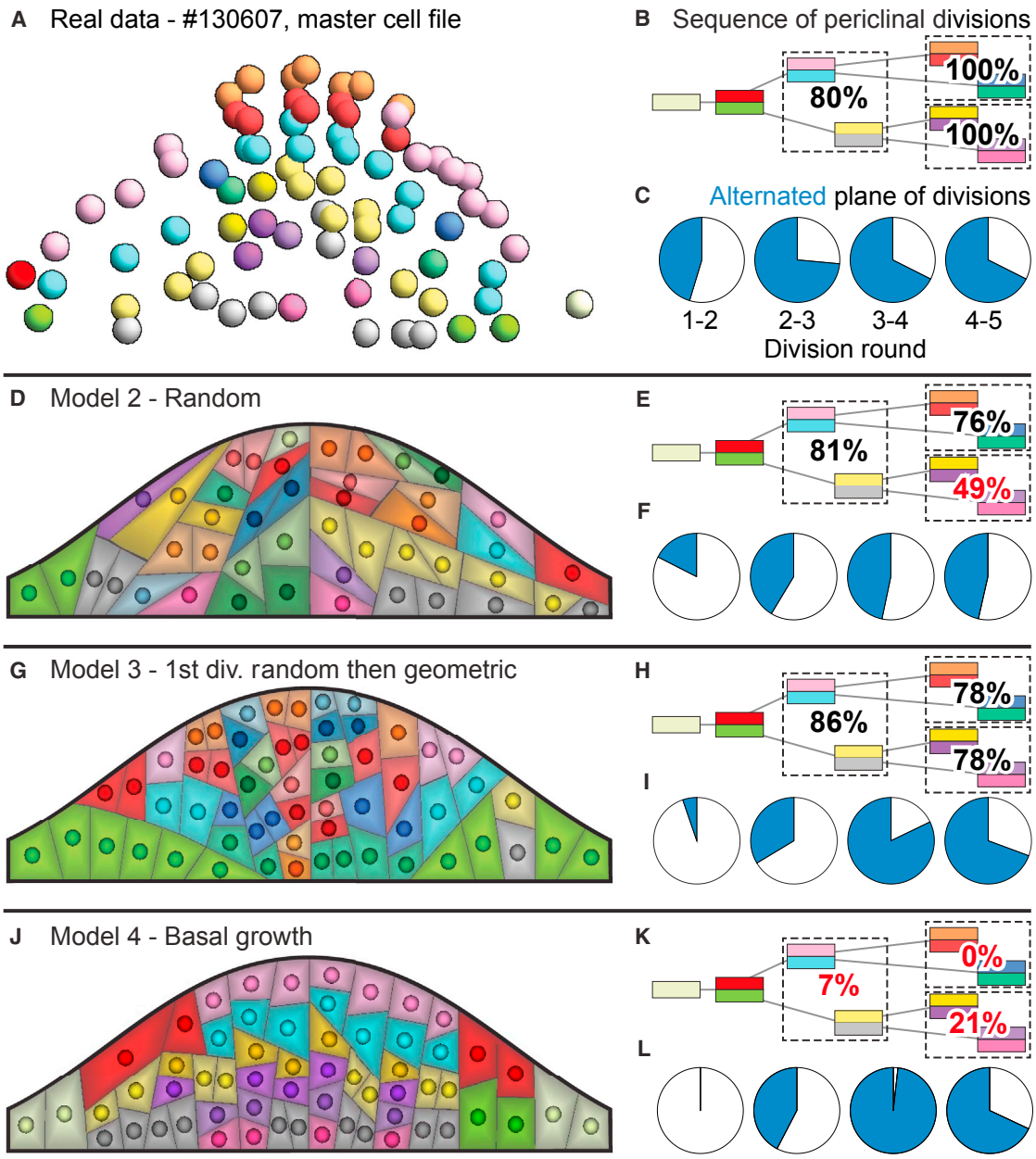

Figure 6. Modeling Lateral Root Morphogenesis

Simulations of lateral root growth using different scenarios of cell divisions (D–L) compared to the real data (A–C). In model 2 (random), cells divide along a randomly chosen division plane (D–F). Model 3 is similar to model 1 (see Figures 1A–1C), but during the first cell division round, the division plane is chosen randomly (G–I). In model 4 (basal growth), lateral root growth is driven by the base (J and K).

(A) Side view of cell nuclei positions in the master cell file of dataset no. 130607 during the final segmented time.

(D, G, and J) Cell outlines overlaid with nuclei show the resulting model at the end of the simulation. Colors indicate layers as in Figure 2D.

(B, E, H, and K) Tree representation of the order of periclinal divisions. Percentages indicate the proportion of periclinal divisions that occur in the outer layer prior to the inner layer for all in vivo datasets (B) or in 100 independent simulation runs of the models (E, H, and K; red font <50%).

(C, F, I, and L) Pie charts representing the proportion of alternating divisions (in blue) in the indicated division rounds for all in vivo datasets (C) or in 100 independent simulation runs of the models (F, I, and L).

See also Figure S7 and Movie S5.

apical-driven growth (Figure 1A), similar to the one empirically observed (Figure 2B), to a growth more pronounced at the base. Importantly, the start and end geometries of the primordium are preserved. Such a model leads to lateral roots qualitatively indistinguishable from the ones with apical growth in terms of layer formation and division orientation (Figures 6J, 6L, and S7). However, base-driven growth impaired the emergence of the periclinal divisions order that we observed in vivo (Figure 6K).

This indicates that the order of periclinal divisions is a result of the growth pattern.

DISCUSSION

By combining whole-organ lineage tracing in wild-type and mutant plants with modeling, we identified the principles governing lateral root morphogenesis. Lateral roots arise from a variable number of founder cells arranged in a field of cells, from which some emerge stochastically and contribute dominantly. Whereas the first asymmetric division of these founders is tightly regulated, the subsequent divisions do not follow a rigid sequence. The orientation of the plane of division depends on the cell geometry. This, combined with the apical growth of the primordium, which results from the proliferation of its constituting cells and the accommodation by the overlying tissue, is instrumental for the emergence of the characteristic layered organization of the primordium. Our model predicts and explains certain patterns of cell divisions (switch in orientation and sequence of periclinal divisions), but the model also misses some of the major features of lateral root formation. It does not reproduce, for example, the precise disposition of cell walls underpinning the organization of the pre-vascular strand, already evident from early stages onward [11]. The mode of lateral root development, in which the organ-level coupling of cell growth and division results in the emergence of a typical pattern, is typical of a non-deterministic, self-organizing system. Self-organization and non-determinism are widespread in developmental processes [36]. Yet, the degree at which these processes are canalized varies. The highly canalized pattern of cell divisions of the early *Arabidopsis* embryo is not prototypic for flowering plants [37]. In contrast, the pattern of cell divisions during post-embryonic formation of lateral root appears in comparison less canalized. Therefore, it will be interesting to identify how self-organization and non-deterministic behavior can be more or less canalized.

EXPERIMENTAL PROCEDURES

Details of experimental procedures are available in the Supplemental Information.

SUPPLEMENTAL INFORMATION

Supplemental Information includes Supplemental Experimental Procedures, seven figures, one table, five movies, and one dataset and can be found with this article online at http://dx.doi.org/10.1016/j.cub.2015.12.047.

AUTHOR CONTRIBUTIONS

D.v.W. acquired all microscopy datasets. J.F. performed all simulations and wrote the Supplemental Information with support from R.S.S. Data analysis was performed by D.v.W., J.F., A.S., H.L., A.M., and E.H.K.S. A.M. wrote the paper with contributions of all authors.

ACKNOWLEDGMENTS

We thank M.J. Bennett, L. Laplaze, and S. Lemke for their helpful comments. This work was supported by the Land Baden-Württemberg, the Chica und Heinz Schaller Stiftung, the CellNetworks cluster of excellence, and the Boehringer Ingelheim Fond (to J.F. and A.M.) and the Cluster of Excellence "Macromolecular Complexes" at the Goethe University Frankfurt am Main (CEF-MC II; DFG Project EXC 115; to D.v.W., A.S., and E.H.K.S.).

Received: October 20, 2015
Revised: November 18, 2015
Accepted: December 9, 2015
Published: January 28, 2016

REFERENCES

1. Yoshida, S., Barbier de Reuille, P., Lane, B., Bassel, G.W., Prusinkiewicz, P., Smith, R.S., and Weijers, D. (2014). Genetic control of plant development by overriding a geometric division rule. Dev. Cell *29*, 75–87.
2. De Smet, I., Lau, S., Mayer, U., and Jürgens, G. (2010). Embryogenesis - the humble beginnings of plant life. Plant J. *61*, 959–970.
3. Gooh, K., Ueda, M., Aruga, K., Park, J., Arata, H., Higashiyama, T., and Kurihara, D. (2015). Live-cell imaging and optical manipulation of Arabidopsis early embryogenesis. Dev. Cell *34*, 242–251.
4. Malamy, J.E. (2005). Intrinsic and environmental response pathways that regulate root system architecture. Plant Cell Environ. *28*, 67–77.
5. Bao, Y., Aggarwal, P., Robbins, N.E., 2nd, Sturrock, C.J., Thompson, M.C., Tan, H.Q., Tham, C., Duan, L., Rodriguez, P.L., Vernoux, T., et al. (2014). Plant roots use a patterning mechanism to position lateral root branches toward available water. Proc. Natl. Acad. Sci. USA *111*, 9319–9324.
6. Van Norman, J.M., Xuan, W., Beeckman, T., and Benfey, P.N. (2013). To branch or not to branch: the role of pre-patterning in lateral root formation. Development *140*, 4301–4310.
7. Casimiro, I., Marchant, A., Bhalerao, R.P., Beeckman, T., Dhooge, S., Swarup, R., Graham, N., Inzé, D., Sandberg, G., Casero, P.J., and Bennett, M. (2001). Auxin transport promotes Arabidopsis lateral root initiation. Plant Cell *13*, 843–852.
8. Swarup, K., Benková, E., Swarup, R., Casimiro, I., Péret, B., Yang, Y., Parry, G., Nielsen, E., De Smet, I., Vanneste, S., et al. (2008). The auxin influx carrier LAX3 promotes lateral root emergence. Nat. Cell Biol. *10*, 946–954.
9. Vermeer, J.E., von Wangenheim, D., Barberon, M., Lee, Y., Stelzer, E.H., Maizel, A., and Geldner, N. (2014). A spatial accommodation by neighboring cells is required for organ initiation in Arabidopsis. Science *343*, 178–183.
10. Lucas, M., Kenobi, K., von Wangenheim, D., Voβ, U., Swarup, K., De Smet, I., Van Damme, D., Lawrence, T., Péret, B., Moscardi, E., et al. (2013). Lateral root morphogenesis is dependent on the mechanical properties of the overlaying tissues. Proc. Natl. Acad. Sci. USA *110*, 5229–5234.
11. Malamy, J.E., and Benfey, P.N. (1997). Organization and cell differentiation in lateral roots of Arabidopsis thaliana. Development *124*, 33–44.
12. Errera, L. (1886). Sur une condition fondamentale d'équilibre des cellules vivantes. Comptes Rendus Hebdomadaires Des Seances De lAcademie *103*, 822–824.
13. Minc, N., and Piel, M. (2012). Predicting division plane position and orientation. Trends Cell Biol. *22*, 193–200.
14. Besson, S., and Dumais, J. (2011). Universal rule for the symmetric division of plant cells. Proc. Natl. Acad. Sci. USA *108*, 6294–6299.
15. Smith, R.S., and Bayer, E.M. (2009). Auxin transport-feedback models of patterning in plants. Plant Cell Environ. *32*, 1258–1271.
16. Vilches-Barro, A., and Maizel, A. (2015). Talking through walls: mechanisms of lateral root emergence in Arabidopsis thaliana. Curr. Opin. Plant Biol. *23*, 31–38.
17. Lavenus, J., Goh, T., Guyomarc'h, S., Hill, K., Lucas, M., Voß, U., Kenobi, K., Wilson, M.H., Farcot, E., Hagen, G., et al. (2015). Inference of the Arabidopsis lateral root gene regulatory network suggests a bifurcation mechanism that defines primordia flanking and central zones. Plant Cell *27*, 1368–1388.
18. Buckingham, M.E., and Meilhac, S.M. (2011). Tracing cells for tracking cell lineage and clonal behavior. Dev. Cell *21*, 394–409.

19. Amat, F., and Keller, P.J. (2013). Towards comprehensive cell lineage reconstructions in complex organisms using light-sheet microscopy. Dev. Growth Differ. *55*, 563–578.

20. Kurup, S., Runions, J., Köhler, U., Laplaze, L., Hodge, S., and Haseloff, J. (2005). Marking cell lineages in living tissues. Plant J. *42*, 444–453.

21. Huisken, J., Swoger, J., Del Bene, F., Wittbrodt, J., and Stelzer, E.H. (2004). Optical sectioning deep inside live embryos by selective plane illumination microscopy. Science *305*, 1007–1009.

22. Keller, P.J., Schmidt, A.D., Wittbrodt, J., and Stelzer, E.H.K. (2008). Reconstruction of zebrafish early embryonic development by scanned light sheet microscopy. Science *322*, 1065–1069.

23. Maizel, A., von Wangenheim, D., Federici, F., Haseloff, J., and Stelzer, E.H. (2011). High-resolution live imaging of plant growth in near physiological bright conditions using light sheet fluorescence microscopy. Plant J. *68*, 377–385.

24. Höckendorf, B., Thumberger, T., and Wittbrodt, J. (2012). Quantitative analysis of embryogenesis: a perspective for light sheet microscopy. Dev. Cell *23*, 1111–1120.

25. Stelzer, E.H.K. (2015). Light-sheet fluorescence microscopy for quantitative biology. Nat. Methods *12*, 23–26.

26. De Rybel, B., Vassileva, V., Parizot, B., Demeulenaere, M., Grunewald, W., Audenaert, D., Van Campenhout, J., Overvoorde, P., Jansen, L., Vanneste, S., et al. (2010). A novel aux/IAA28 signaling cascade activates GATA23-dependent specification of lateral root founder cell identity. Curr. Biol. *20*, 1697–1706.

27. Laskowski, M., Grieneisen, V.A., Hofhuis, H., Hove, C.A.T., Hogeweg, P., Marée, A.F.M., and Scheres, B. (2008). Root system architecture from coupling cell shape to auxin transport. PLoS Biol. *6*, e307.

28. Lucas, M., Godin, C., Jay-Allemand, C., and Laplaze, L. (2008). Auxin fluxes in the root apex co-regulate gravitropism and lateral root initiation. J. Exp. Bot. *59*, 55–66.

29. Laskowski, M.J., Williams, M.E., Nusbaum, H.C., and Sussex, I.M. (1995). Formation of lateral root meristems is a two-stage process. Development *121*, 3303–3310.

30. Dubrovsky, J.G., Rost, T.L., Colón-Carmona, A., and Doerner, P. (2001). Early primordium morphogenesis during lateral root initiation in Arabidopsis thaliana. Planta *214*, 30–36.

31. Voß, U., Wilson, M.H., Kenobi, K., Gould, P.D., Robertson, F.C., Peer, W.A., Lucas, M., Swarup, K., Casimiro, I., Holman, T.J., et al. (2015). The circadian clock rephases during lateral root organ initiation in Arabidopsis thaliana. Nat. Commun. *6*, 7641.

32. Graner, F., Dollet, B., Raufaste, C., and Marmottant, P. (2008). Discrete rearranging disordered patterns, part I: robust statistical tools in two or three dimensions. Eur Phys J E Soft Matter *25*, 349–369.

33. Goh, T., Joi, S., Mimura, T., and Fukaki, H. (2012). The establishment of asymmetry in Arabidopsis lateral root founder cells is regulated by LBD16/ASL18 and related LBD/ASL proteins. Development *139*, 883–893.

34. Robinson, S., Barbier de Reuille, P., Chan, J., Bergmann, D., Prusinkiewicz, P., and Coen, E. (2011). Generation of spatial patterns through cell polarity switching. Science *333*, 1436–1440.

35. Van Damme, D., De Rybel, B., Gudesblat, G., Demidov, D., Grunewald, W., De Smet, I., Houben, A., Beeckman, T., and Russinova, E. (2011). Arabidopsis α Aurora kinases function in formative cell division plane orientation. Plant Cell *23*, 4013–4024.

36. Camazine, S. (2003). Self-organization in Biological Systems (Princeton University Press).

37. Steeves, T.A., and Sussex, I.M. (1989). Patterns in Plant Development (Cambridge University Press).